DALTON
FULL PAPER

Synthesis, electrochemistry, and spectroelectrochemistry of a metalloporphyrin–viologen donor–acceptor diad

Matthew T. Barton,[a] Natalie M. Rowley,*[a] Peter R. Ashton,[a] Christopher J. Jones,[a] Neil Spencer,[a] Malcolm S. Tolley[a] and Lesley J. Yellowlees[b]

[a] *School of Chemistry, The University of Birmingham, Edgbaston, Birmingham, UK B15 2TT*
[b] *Department of Chemistry, University of Edinburgh, Edinburgh, UK EH9 3JJ*

Received 10th May 2000, Accepted 10th July 2000
Published on the Web 24th August 2000

A new donor–acceptor (D–A) molecule, zinc 5-{*N*-[4-(1′-benzyl-4,4′-bipyridinium-1-ylmethyl)benzyl]-4-pyridinio}-10,15,20-triphenylporphyrinate tris(hexafluorophosphate) has been synthesized. The diad and its precursors have fully been characterised by ^{1}H and ^{13}C NMR spectroscopy, mass spectrometry, UV/Visible spectroscopy and cyclic voltammetry. *In situ* UV/Visible and EPR measurements show that the site of the first and second electrochemical reductions is the benzyl viologen component of the molecule, whilst the third electron reduction process is associated with the porphyrin moiety. The first reduction process gave rise to an EPR signal due to the benzyl viologen radical, whilst the second caused the molecule to become diamagnetic. The third of these processes gave rise to a new EPR signal, which was found to correspond to the metalloporphyrin radical.

There has been much interest in artificial models of photoinduced electron transfer, and covalently linked porphyrin–viologen molecules have featured heavily in this work.[1,2] Systems have been extensively studied photochemically, electrochemically and spectroelectrochemically, but we are not aware of detailed *in situ* EPR studies, which is the primary focus of this paper. Wrighton and co-workers[2] have previously demonstrated that pulsed laser excitation (354.7 nm, 10 ns pulse) of a pyridyltritolylporphyrin chromophore covalently linked to a dibenzyl viologen, Bz_2V^{2+}, electron acceptor (porphyrin–viologen, P–V^{2+}) in acetonitrile led to intramolecular electron transfer quenching of the porphyrin singlet excited state within the laser pulsewidth to reduce the linked Bz_2V^{2+} to $Bz_2V^{+\bullet}$. Transient $Bz_2V^{+\bullet}$ was detected directly by resonance Raman spectroscopy. Confirmation of the assignment of the transient $Bz_2V^{+\bullet}$ came from comparison of the spectra with that of an authentic sample of $Bz_2V^{+\bullet}$, and of electrochemically reduced P–V^{2+}, which was spectroscopically confirmed to form P–$V^{+\bullet}$. Fluorescence lifetime determinations for P–V^{2+} and P gave a rate constant for intramolecular electron transfer, $k_{et} = 8 \times 10^7$ s^{-1}, consistent with the ability to observe electron transfer within the laser pulsewidth. More recently, Yonemoto *et al.*[3] have shown that donor–acceptor complexes of the type [(2,2′-bipyridine)$_2$Ru(4-CH_3-2,2′-bipyridine-4′)–$(CH_2)_n$–(4,4′-bipyridinium-CH_3)]$^{4+}$ (n = 2–5, 7, 8) can be exchanged onto the surface of large-pore zeolites (Y, L and mordenite). From solid state CP-MAS spectra of ^{13}C-labelled compounds, it was established that these diads occupy surface sites, in which the acceptor end is occluded by the zeolite channels, while the size-excluded donor end is exposed. It was also found that the back electron transfer reaction is approximately 10^5 times slower for diads on the zeolite surface than in solution.

We have previously synthesized a series of peripherally metallated porphyrins and reported their photochemical properties.[4–6] Following on from our earlier work, we wished to develop new systems which give rise to longer lifetimes of the photoinduced charge-separated states, with a view to using the phototransferred electron to carry out a further chemical reduction. In order to achieve this, we constructed diad systems capable of occlusion by zeolite Y, in the hope that our systems would behave in a similar manner to those of Yonemoto *et al.*[3] In the first step towards our goal we have recently reported the synthesis, electrochemistry and spectroelectrochemistry of a new donor–acceptor (D–A) molecule, 5-{*N*-[4-(1′-benzyl-4,4′-bipyridinium-1-ylmethyl)benzyl]-4-pyridinio}-10,15,20-triphenylporphyrin tris(hexafluorophosphate).[7]

In this paper we report the synthesis, characterisation, electrochemistry and spectroelectrochemistry of a new, but related metalloporphyrin-based donor–acceptor compound and its precursors. The target molecule comprises a metalloporphyrin, covalently attached to a dibenzyl viologen acceptor unit, the acceptor end of which is sufficiently small to be occluded by large pore zeolites, such as zeolite Y. Although the diad described here is closely related to that studied previously by Wrighton and co-workers,[2] it is a new compound and has been characterised by more detailed spectroelectrochemical studies and low temperature *in situ* EPR studies.

Results and discussion

Synthesis

Porphyrin **1** was prepared by an Adler-type condensation of pyrrole, benzaldehyde and pyridine-4-carbaldehyde.[7,8] Compound **2** was prepared in high yield by treatment of **1** in chloroform with zinc acetate in methanol.[9] Compound **3** was prepared by quaternisation of the pyridyl moiety of **2** with an excess of α,α′-dibromo-*p*-xylene. The synthesis of compound **4** has previously been described.[7] Further reaction of **3** with **4**, followed by counter-ion exchange, afforded the desired diad **5**. ^{1}H NMR spectroscopy, liquid secondary ion mass spectrometry (LSIMS) and elemental analyses confirm the identity of all of the reported compounds.

^{1}H NMR Spectra

In general, the ^{1}H NMR spectra of compounds **1**–**5** were well resolved and could easily be assigned. Large shifts were seen due to the presence of quaternised nitrogen atoms and the ring-current effect of the porphyrin macrocycle. These generally shifted signals to very high frequency, except for internal

 DOI: 10.1039/b003738i

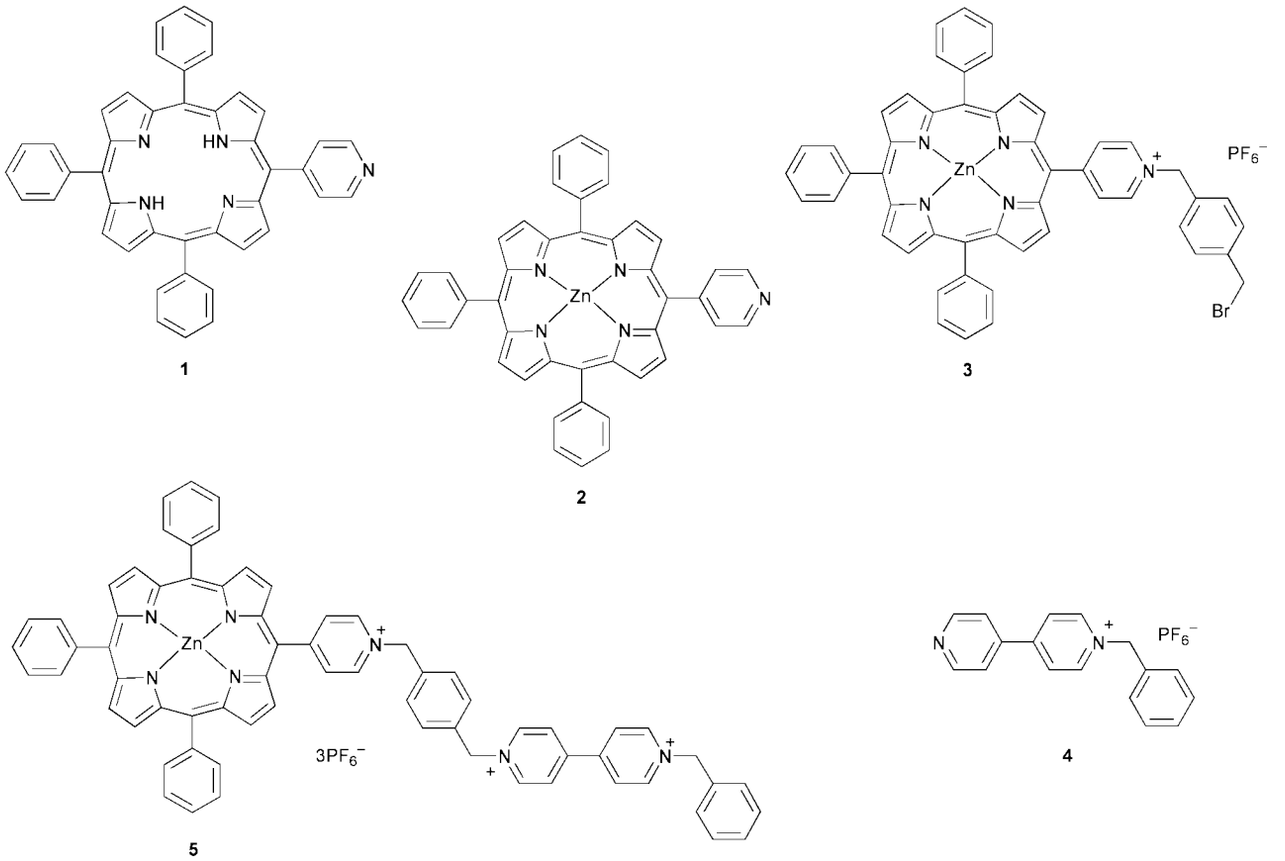

porphyrin NH protons which were shifted to low frequency by the ring current.

^{13}C NMR Spectra

The spectrum of compound **5** has partially been assigned by means of 2-dimensional NMR [heteronuclear single quantum coherence (HSQC)] and PENDANT[15] experiments. The assignment of quaternary carbon environments is incomplete (peaks listed in curly brackets in Experimental section).

Electronic absorption spectra

The electronic spectral data for compounds **1**–**5** are shown in Table 1. In dichloromethane the porphyrin-based compounds show absorption spectra characteristic of the porphyrin moiety. Compound **1**,[7] an unmetallated porphyrin, shows the expected five major absorptions: the intense B or Soret band at 415 nm, and four Q bands in the range 500–650 nm which decrease in intensity with increasing wavelength. The electronic spectra of the metallated porphyrin compounds show the characteristic Soret band and only two Q bands, due to increased symmetry. Compound **3** shows an additional absorption at 233 nm, corresponding to the xylene moiety. The absorption due to the acceptor component (266 nm for compound **4**) combines with the xylene absorption to give a broader band at 256 nm when present in **5**.

There is small perturbation in the positions of the Q bands of compound **5**, compared to those of the individual components, indicating the possibility of a small amount of ground state electronic interaction between the components of the diad, when assembled.

Cyclic voltammetry

The electrochemical properties of compounds **1**–**5** were examined by cyclic voltammetry in dry dichloromethane using a platinum bead working electrode and [*n*-Bu_4N][BF_4] as supporting electrolyte (Table 2). The electrochemistry of compound **5** was also studied in acetonitrile solution. In general, porphyrins are expected to undergo two reduction and two oxidation processes, each consistent with a one-electron transfer reaction. Compound **1**[7] shows two chemically reversible reductions in the expected range and one irreversible oxidation, all associated with the porphyrin macrocycle. Presumably the second oxidation expected for a porphyrin is masked by solvent breakdown (*i.e.* beyond around +1.50 V).

The zincated analogue of **1**, compound **2**, exhibits two reductions (−1.26 and −1.55 V *vs*. SCE). The first is chemically reversible, whilst the second is irreversible leading to the formation of a new product wave at −0.40 V. Compound **2** also has three irreversible oxidation processes (+0.94, +1.24 and +1.52 V). All of the waves are at more negative potential when compared to those of the non-zincated compound, an effect which has been observed previously when inserting zinc into a porphyrin macrocycle.[10] Two oxidation processes are expected for a porphyrin, and it is possible that the additional third oxidation process which is observed here is due to isoporphyrin formation.[11]

Compound **3** exhibits three oxidation processes, at similar potentials to those of **2** and assigned as above for **2**. It also exhibits two reduction processes. That at −0.84 V is irreversible and probably associated with the pyridinium porphyrin entity, being similar in potential to the third reduction potential observed for compound **5** (see below). Compound **4** exhibits two reduction processes at −0.76 and −1.47 V.

The electrochemistry of compound **5** was investigated by cyclic voltammetry in both dichloromethane and acetonitrile. The cyclic voltammograms were generally similar, showing two oxidation and four reduction processes in each case. However, the compound was poorly soluble in dichloromethane, and the second reduction process appeared to be associated with some electrode coating. This problem was not found with acetonitrile as solvent, and so the interpretation of the electrochemical data is based on our observations with acetonitrile solutions.

In acetonitrile, two oxidation processes are observed. The first is assigned to the porphyrin entity. It is at a potential

Table 1 Electronic spectral data in dichloromethane for compounds **1**–**5**

Compound	B $\lambda^a(\varepsilon)^b$	$Q_y(1,0)$ $\lambda^a(\varepsilon)^c$	$Q_y(0,0)$ $\lambda^a(\varepsilon)^d$	$Q_x(1,0)$ $\lambda^a(\varepsilon)^d$	$Q_x(0,0)$ $\lambda^a(\varepsilon)^d$	$\lambda^a(\varepsilon)^c$
1[7]	415 (2.4)	513 (1.7)	547 (6.5)	587 (4.6)	644 (2.7)	
2	416 (2.4)	561 (1.4)[e]	604 (4.3)[f]			
3	414 (1.5)	556 (8.7)[d,e]	600 (6.0)[f]			233 (2.3)
4[7]						266 (5.2)
5	415 (2.2)	559 (1.7)[e]	621 (1.5)[c,f]			256 (6.8)

[a] In nm. [b] In L mol^{-1} cm^{-1} × 10^5. [c] In L mol^{-1} cm^{-1} × 10^4. [d] In L mol^{-1} cm^{-1} × 10^3. [e] Q(1,0). [f] Q(0,0).

Table 2 Electrochemical data obtained for compounds **1**–**5**[a]

Compound	Solvent	Oxidation, E_f/V			Reduction, E_f/V (ΔE_p/mV)			
1[7]	CH_2Cl_2	+1.16[b]			−1.05 (100)	−1.40 (100)		
2	CH_2Cl_2	+0.94[b]	+1.24[b]	+1.52[b]	−1.26 (130)	−1.55[b]		
3	CH_2Cl_2	+1.01[b]	+1.25[b]	+1.46[b]	−0.84[b]	−1.72[b]		
4[7]	CH_2Cl_2				−0.76 (109)	−1.47 (160)		
5	CH_2Cl_2	+0.97[b]	+1.46[b]		−0.18 (71)	−0.67[b,c]	−0.88[b]	−1.62[b]
5	MeCN	+0.96[b]	+1.21[b]		−0.32 (72)	−0.73 (61)	−0.95 (56)	−1.78[b]

[a] All measurements were made by cyclic voltammetry, in the solvent specified, containing 0.2 mol dm^{-3} [*n*-Bu_4N][BF_4] at a platinum bead working electrode. The scan rate was 200 mV s^{-1}. All potentials are *vs.* SCE. The ferrocenium–ferrocene couple was used as an internal reference (E_f = 0.55 ± 0.01 V in dichloromethane, 0.46 ± 0.01 V in acetonitrile). Values in parentheses are peak–peak separations for the reversible processes (ΔE_p for the ferrocenium–ferrocene couple under the same conditions was about 90 ± 30 mV in dichloromethane and 70 ± 10 mV in acetonitrile). [b] Irreversible process. [c] This reduction appeared to be associated with some other process, possibly electrode coating.

comparable with that of compound **2** and is irreversible. The second oxidation is therefore presumably due to the decomposition product of the first oxidation process. The first reduction appears at −0.32 V in acetonitrile. This reversible process has been assigned by other methods to the acceptor moiety of the molecule (see below). The solvent dependence of the first reduction process indicates that the dibenzyl viologen moiety must interact with the solvent. The second reduction process is also reversible in acetonitrile (−0.73 V) and is assigned to the dibenzyl viologen moiety. *In situ* EPR experiments demonstrate that the first two reduction processes are closely associated with each other (see below). The third (reversible) and fourth (irreversible) reduction processes are both assigned to porphyrin based electron transfer.

For the analogous non-zincated diad[7] it was found that the second and third reduction processes were at very similar potentials, and unresolved by cyclic voltammetry under equivalent conditions. It has already been noted (see above) that adding zinc to a porphyrin ring causes a negative shift in all electrochemical processes associated with the macrocycle. When comparing the zincated and free-base diads, both the first and second dibenzyl viologen reductions appear at similar potentials, whereas the first and second porphyrin reductions are seen at different potentials. Thus two waves may be resolved for the zincated diad which were unresolved for the free-base diad.

Spectroelectrochemistry

In situ electronic absorption spectra of compound **5** were recorded in a 0.1 mol dm^{-3} solution of [*n*-Bu_4N][BF_4] in dry acetonitrile at 253 K. From cyclic voltammetry, three reversible reduction processes are seen, at −0.32, −0.73 and −0.95 V, and these were further investigated. The irreversible reduction process at −1.78 V was not investigated.

During the first reduction (Fig. 1), when the potential is set to −0.50 V, small changes are seen in the Soret band and the two Q bands of the porphyrin moiety. The bands shift to higher wavelength (by around 30 nm) and there is some collapse in intensity, notably in the Soret band. The band at 260 nm decreases, a shoulder develops at 320 nm, and a new, broad absorption is seen at around 890 nm (Fig. 2). This

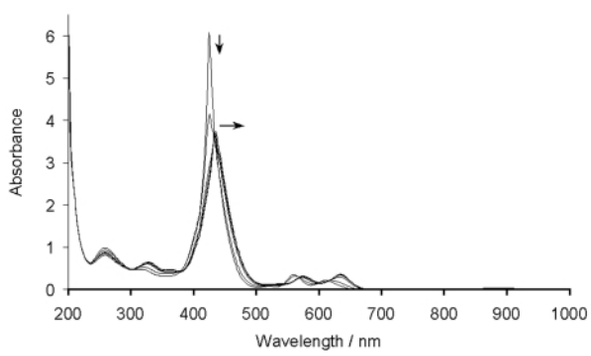

Fig. 1 Electronic spectra recorded during reduction of compound **5** to **5**$^-$ showing the collapse of the Soret band.

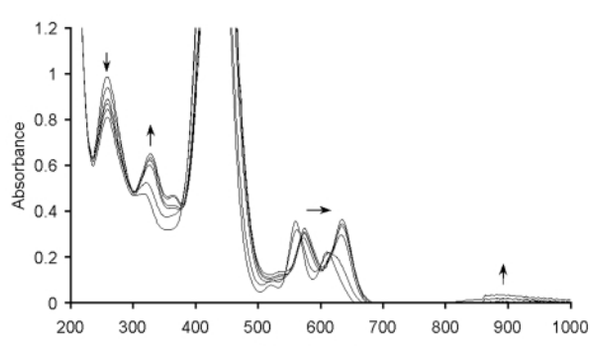

Fig. 2 Electronic spectra recorded during reduction of compound **5** to **5**$^-$.

first reduction process is therefore assigned to the acceptor component of the molecule, and is reversible under these conditions since the original spectrum is recovered by returning the potential to +0.20 V. Since the porphyrin bands also change slightly at this potential, it would appear that there is also some degree of porphyrin involvement in the reduction. In contrast, it was previously found[7] that the analogous free-base diad did not exhibit any significant amount of porphyrin involvement in the equivalent first reduction.

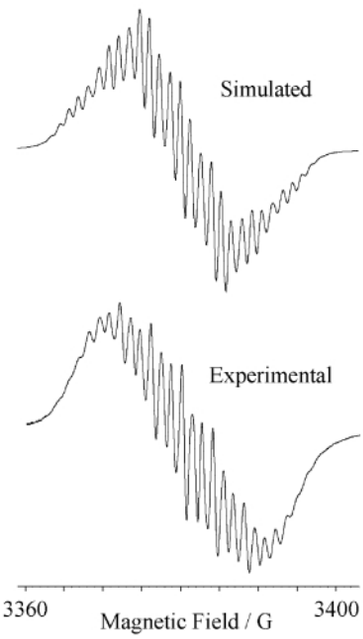

Fig. 3 *In situ* EPR spectrum recorded during reduction of compound **5** to $\mathbf{5}^{-}$ at −0.50 V in DMF at 233 K and simulated EPR spectrum. Simulation of $\mathbf{5}^{-}$ used parameters in the text with a Lorentzian linewidth of 1.1 G.

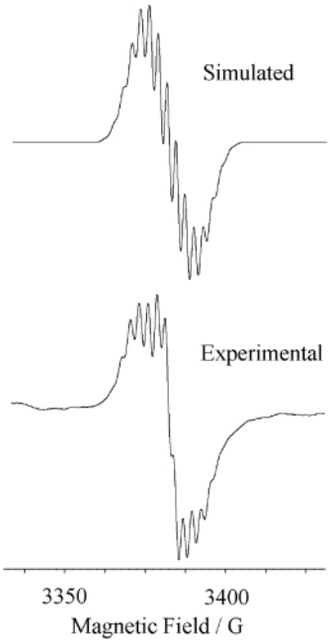

Fig. 4 *In situ* EPR spectrum recorded during reduction of compound $\mathbf{5}^{2-}$ to $\mathbf{5}^{3-}$ at −1.52 V in DMF at 233 K and simulated EPR spectrum. Simulation of $\mathbf{5}^{3-}$ used parameters in the text with a Lorentzian linewidth of 2.7 G.

Upon controlled potential reduction at −0.85 V there is little further change to the porphyrin bands, indicating that there is little porphyrin involvement in the site of the second reduction process. This is to be expected since this process is assigned to a dibenzyl viologen reduction. When the potential is set to −1.52 V there is a dramatic change in the UV/Visible spectrum of compound **5**. A strong new absorption develops at around 480 nm and the characteristic Q bands are almost totally bleached. A broad absorbance is seen centred on 1000 nm. This process is irreversible under these conditions, since the original spectrum cannot be reproduced by setting the potential back to +0.2 V, and is assigned as a porphyrin-based reduction.

EPR Spectral studies

The site of the first reduction process of compound **5** was confirmed using *in situ* EPR spectroscopy in a 1.0 mol dm^{-3} solution of [*n*-Bu_4N][BF_4] in DMF at 233 K. When the controlled potential is set to −0.50 V a signal develops at $g = 2.012$ which is indicative of the formation of a radical species (Fig. 3). The signal shows around 27 resolved lines. Simulations (Fig. 3) demonstrate that this is attributed to coupling of the unpaired electron with three N atoms (we infer then that these are the acceptor N atoms, $a^{N} = 4.01$ G), six H atoms ($a^{H} = 1.30$ G) and a further six H atoms ($a^{H} = 1.00$ G). Consideration of the structure of **5** would suggest that the redox process at −0.32 V should be attributed to the acceptor part of the compound which has three equivalent nitrogen sites (the porphyrin ring having four equivalent nitrogen sites). It is likely that six H atoms observed in the EPR spectrum are methylene protons (2 per nitrogen) and six are aromatic protons (again 2 per nitrogen) adjacent to N, although we cannot discount all twelve H atoms being aromatic protons, and hence a detailed assignment of EPR coupling to specific H atoms requires further study. This demonstrates that the dibenzyl viologen moiety is the first site of reduction, and therefore the most likely receptor for the transferred electron in the photoinduced electron transfer process.

On application of a potential of −0.85 V the EPR signal decays as the system becomes diamagnetic. Since the two electrochemically added electrons are pairing up in this way they must be strongly coupled on the molecule. Therefore this second reduction is also assigned to the acceptor end of the molecule.

At −1.52 V a new signal develops (Fig. 4) as a third electron is added to the molecule. This EPR signal has 13 lines and is centred at $g = 2.011$. In this case, simulations (Fig. 4) show that the signal shape may be modelled by coupling of the unpaired electron to four equivalent N atoms (presumably porphyrin-based, $a^{N} = 2.65$ G), one further N atom (presumably pyridinium, $a^{N} = 5.40$ G) and two H atoms (exact identity undefined, $a^{H} = 2.7$ G). Reversal of the applied potential to −0.61 V shows collapse of the signal at $g = 2.011$ to give a featureless EPR spectrum and then growth of the first signal at $g = 2.012$. The EPR experiments show that at 233 K compound **5** is stable in redox states $\mathbf{5}^{-}$, $\mathbf{5}^{2-}$ and $\mathbf{5}^{3-}$.

Conclusion

We have described the synthesis and characterisation of a new potentially photoactive donor–acceptor diad, compound **5,** and its precursors. *In situ* UV/Visible and EPR measurements have shown that the site of the first and second electrochemical reductions is the dibenzyl viologen component of the molecule, and that the third reduction process is associated with the porphyrin entity. It appears, however, from *in situ* UV/Visible measurements, that there is a small degree of porphyrin involvement in the first electrochemical reduction process. These findings are in contrast to those for the analogous free base diad,[7] where it was found by *in situ* UV/Visible measurements that the site of the first electrochemical reduction was purely the benzyl viologen component. In addition, the second reduction wave from cyclic voltammetry of the free base analogue was shown by *in situ* EPR to comprise two unresolved one-electron processes. The first reduction process rendered the diad diamagnetic, as was shown by the disappearance of the signal due to the benzyl viologen radical. The second gave rise to the appearance of a new EPR signal, which was found to correspond to the porphyrin radical. For the zinc analogue, reported here, the second and third reduction processes are resolved.

These are significant steps towards our ultimate aim of assembling zeolite-occluded diads in order to attempt the photogeneration of long-lived charge separated states. The results presented here suggest that the photochemistry of the

free base and zincated diads will be different, due to apparent differences in the ground-state electronic interactions between the donor and acceptor components of the diads.

Experimental

General details

All reagents were purchased from Aldrich and used without further purification. Reaction solvents were deoxygenated and dried by standard methods before use. Compounds were purified by column chromatography (column lengths *ca.* 0.3 m) using Kiesel gel 60 (Merck 5554; 70–230 mesh). ^{1}H NMR spectra were recorded using Bruker AC300 (300 MHz) or AMX400 (400 MHz) spectrometers, ^{13}C NMR spectra using Bruker DRX500 (125 MHz) or AMX400 (100 MHz) spectrometers and assignments made using a combination of both PENDANT and HSQC experiments.

Low resolution LSIMS spectra were obtained from a VG Zabspec mass spectrometer utilising a *m*-nitrobenzyl alcohol matrix and scanning in the positive ion mode at a speed of 5 s per decade. Absorption spectra were obtained using a Shimadzu UV-240 spectrophotometer. Solvent background corrections were made in all cases.

Cyclic voltammetry was carried out using an EG & G model 362 potentiostat and the Condecon 310 software package, with *ca.* 10^{-3} mol dm^{-3} solutions under dry N_2 in dry dichloromethane or acetonitrile. A platinum bead working electrode was used, with 0.2 mol dm^{-3} [*n*-Bu_4N][BF_4] as supporting electrolyte, and a scan rate of 200 mV s^{-1}. Potentials were recorded *vs.* a saturated calomel reference electrode, and ferrocene (E_f = 0.55 ± 0.01 V in dichloromethane) was added as an internal standard. The data obtained were reproducible, the experimental error being ±10 mV.

All spectroelectrochemical studies were carried out using an Autolab System containing a PSTAT20 potentiostat, using General Purpose Electrochemical System (GPES) Version 4.5 software. Positive feedback ohmic compensation was applied for all cyclic voltammograms recorded. All solutions were purged with Ar for 20 minutes prior to study. Electrogeneration potentials of the reduction processes were at more negative values than the E_f of the couple.

The optically transparent electrode cell (O.T.E.) for use in UV/vis/near-IR spectrometers has been described previously.[12] EPR spectra were recorded on an X-band Bruker ER200D-SCR spectrometer, using the *in situ* cell described previously.[13] EPR simulations were performed using WINEPR SimFonia.[14]

Microanalyses were performed by the University of North London.

Preparations

5,10,15-Triphenyl-20-(4-pyridyl)porphyrin, 1. The synthesis and characterisation of this compound has been described previously.[7]

Zinc 5,10,15-triphenyl-20-(4-pyridyl)porphyrinate, 2. Compound **1** (0.50 g, 0.81 mmol) was dissolved in chloroform (100 ml) and heated to reflux. Zinc acetate (0.15 g, 0.81 mmol) in methanol (2 ml) was added and the solution heated under reflux for 30 minutes. The resulting solution was evaporated to dryness *in vacuo* and purified by column chromatography, eluting with dichloromethane. The solvent was removed to give compound **2** as a red-purple solid. Yield: 0.41 g (73.6%). ^{1}H NMR (300 MHz, DMSO): δ 8.94 (2 H, d, ^3J = 5.9 Hz, pyridine H_a and $H_{a'}$), 8.78–8.82 (8 H, m, pyrrole protons of rings A, B, C and D), 8.18–8.21 (8 H, overlapping signals, *ortho* protons of Ph and H_b, $H_{b'}$ of pyridine), 7.77–7.82 (9 H, m, *meta* and *para* protons of Ph). Found: C, 76.2, H, 3.9; N, 10.3. Calc. for $C_{43}H_{27}N_5Zn$: C, 76.1; H, 4.0; N, 10.3%. LSIMS: *m*/*z* 678 ([M]$^+$).

Zinc 5-[*N*-(4-bromomethylbenzyl)-4-pyridinio]-10,15,20-triphenylporphyrinate hexafluorophosphate, 3. Compound **2** (0.34 g, 0.5 mmol, 1.0 equivalent) and α,α′-dibromo-*p*-xylene (1.65 g, 6.25 mmol, 12.5 equivalents) were dissolved in dry THF (100 ml) and heated to reflux under nitrogen for 6 hours. The reaction mixture was then left to cool with stirring for 18 hours. The resulting solution was evaporated to half of its original volume *in vacuo*, and then a saturated solution of NH_4PF_6 was added until no further precipitation was seen. The mixture was filtered under vacuum and allowed to air-dry. The crude product was separated from residual starting materials by column chromatography, eluting with 1% methanol in dichloromethane (2.5 L). The solvent was removed to afford **3** as a purple solid. Yield: 0.20 g (38.9%). ^{1}H NMR (300 MHz, CD_3CN): δ 9.03 (2 H, d, ^3J = 6.3, pyridine ring H_a and $H_{a'}$), 8.93 (4 H, A_2B_2, J_{AB} = 4.8, $\Delta\delta_{AB}$ = 0.08 ppm, pyrrole protons of rings A and B), 8.84 (4 H, A_2B_2, J_{AB} = 4.8, $\Delta\delta_{AB}$ = 0.02 ppm, pyrrole rings C and D), 8.77 (2 H, d, ^3J = 6.6, pyridine ring H_b and $H_{b'}$), 8.18–8.22 (6 H, m, *ortho* protons of Ph in porphyrin), 7.75–7.83 (9 H, m, *meta* and *para* protons of Ph in porphyrin), 7.69 (4 H, A_2B_2, J_{AB} = 8.5 Hz, $\Delta\delta_{AB}$ = 0.04 ppm, phenyl ring E), 5.97 (2 H, s, H_c and $H_{c'}$) and 4.69 (2 H, s, H_d and $H_{d'}$). Found: C, 60.8; H, 3.5; N, 7.0. Calc. for $C_{51}H_{35}BrF_6N_5PZn$: C, 60.8; H, 3.5; N, 7.0%. LSIMS: *m*/*z* 862 ([M − PF_6]$^+$), 782 ([M − Br − PF_6]$^+$) and 677 ([M − ($CH_2C_6H_4CH_2Br$) − PF_6]$^+$).

1-Benzyl-4-(4-pyridyl)pyridiniumhexafluorophosphate, 4. The synthesis and characterisation of this compound have been described previously.[7]

Compound 5 (Fig. 5). Compounds **3** (0.10 g, 1.06 × 10^{-4} mol, 1.0 equivalent) and **4** (0.55 g, 1.4 × 10^{-3} mol, 14.0 equivalents) were dissolved in dry acetonitrile (100 ml). The mixture was stirred under reflux for 12 hours under an atmosphere of nitrogen and then left to cool. The volume of the resulting solution was reduced to half under vacuum, then a saturated solution of NH_4PF_6 was added until no further precipitation was seen. The crude product was collected by vacuum filtration and purified by column chromatography (methanol,

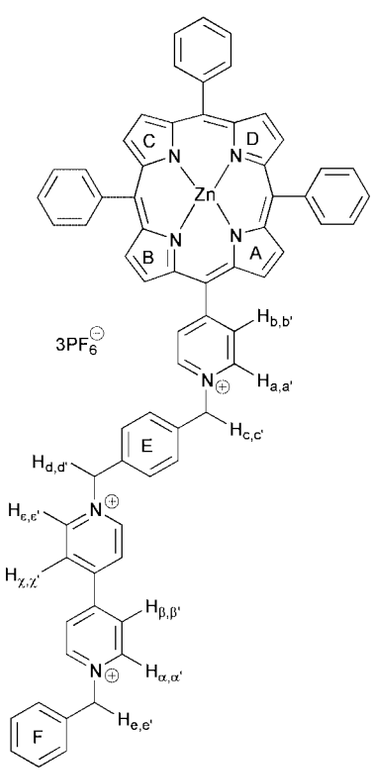

Fig. 5 Atom labelling in diad **5**.

$NH_4^+Cl^-_{(aq)}$ [2.0 mol dm^{-3}], nitromethane; ratio of 7:2:1). The desired product was collected as the major coloured band. Solvent was removed under vacuum and residual solid NH_4^+-Cl^- removed by washing with water. The product was dissolved in dichloromethane and dried over $MgSO_4$. The pure product was obtained as a red-purple solid. Yield: 0.10 g (63.2%). ^{1}H NMR (400 MHz, d_6-acetone): δ 9.56 (2 H, d, ^3J = 6.6, H_a and $H_{a'}$ of porphyrin pyridine ring), 9.51 (2 H, d, ^3J = 6.8, H_ε and $H_{\varepsilon'}$ of 4,4′-bipyridine), 9.46 (2 H, d, ^3J = 7.0, H_α and $H_{\alpha'}$ of 4,4′-bipyridine), 9.03 (2 H, d, ^3J = 6.5, H_b and $H_{b'}$ of porphyrin pyridine ring), 8.97 (4 H, A_2B_2, J_{AB} = 4.8, $\Delta\delta_{AB}$ = 0.05 ppm, pyrrole protons of rings A and B), 8.88 (4 H, A_2B_2, J_{AB} = 4.8, $\Delta\delta_{AB}$ = 0.02 ppm, pyrrole protons of rings C and D), 8.77–8.81 (4 H, m, H_χ,$H_{\chi'}$ and H_β,$H_{\beta'}$ of 4,4′-bipyridine), 8.19–8.21 (6 H, m, *ortho* protons of Ph in porphyrin), 7.99 (4 H, A_2B_2, J_{AB} = 8.5 Hz, $\Delta\delta_{AB}$ = 0.11 ppm, phenyl ring E), 7.78–7.93 (9 H, m, *meta* and *para* protons of Ph in porphyrin), 7.64–7.65 (2 H, m, *ortho* protons of phenyl ring F), 7.48–7.49 (3 H, m, *meta* and *para* protons of phenyl ring F), 6.40 (2 H, s, H_c and $H_{c'}$), 6.29 (2 H, s, H_d and $H_{d'}$) and 6.14 (2 H, s, H_e and $H_{e'}$). ^{13}C NMR (100 MHz, CD_3CO): δ 64.3 ($C[H_c]_2$), 65.1 ($C[H_d]_2$), 65.7 ($C[H_e]_2$), {112.3, 121.7, 122.9}, 126.4, 126.5, 127.6 and 127.7 (*meta* and *para* *C*H of Ph in porphyrin), 129.2 and 129.4 (*C*H of phenyl ring F), 129.2 and 130.1 (*C*H of pyrrole rings A and B), 130.4 and 130.8 (*C*H of phenyl ring E), 131.8 and 132.2 (*C*H of pyrrole rings C and D), 132.9 and 135.1 (*C*H of pyrrole rings A and B), 133.5 (CH_b of porphyrin pyridine ring), 134.2 (*ortho* *C*H of Ph in porphyrin), 134.8, 135.1, 142.5, 142.7, 142.8, 146.0, 148.0, 149.9, 150.1, 150.7 and 161.6. Found: C, 55.8; H, 3.4; N, 6.5. Calc. for $C_{68}H_{50}F_{18}N_7P_3Zn$: C, 55.7; H, 3.4; N, 6.7%. LSIMS: *m*/*z* 1318 ($[M - PF_6]^+$), 1174 ($[M - 2PF_6]^+$) and 677 ($[\mathbf{2}]^+$).

Acknowledgements

We thank the EPSRC (UK) for financial support.

References

1 For example: A. Harriman, G. Porter and A. Wilowska, *J. Chem. Soc.*, *Faraday Trans. 2*, 1984, 191; G. Blondeel, D. De Keukeleire, A. Harriman and L. R. Milgrom, *Chem. Phys. Lett.*, 1985, **118**, 77; I. Okura and H. Hosono, *Inorg. Chim. Acta*, 1991, **189**, 145 and references therein.
2 R. J. McMahon, R. K. Forcé, H. H. Patterson and M. S. Wrighton, *J. Am. Chem. Soc.*, 1988, **110**, 2670; R. K. Forcé, R. J. McMahon, J. Yu and M. S. Wrighton, *Spectrochim. Acta*, *Part A*, 1989, **45**, 23 and references therein.
3 E. H. Yonemoto, Y. I. Kim, R. H. Schmehl, J. O. Wallin, B. A. Shoulders, B. R. Richardson, J. F. Haw and T. E. Mallouk, *J. Am. Chem. Soc.*, 1994, **116**, 10557.
4 N. M. Rowley, S. S. Kurek, M. W. George, P. D. Beer, S. M. Hubig, C. J. Jones, J. M. Kelly and J. A. McCleverty, *J. Chem. Soc.*, *Chem. Commun.*, 1992, 497.
5 N. M. Rowley, S. S. Kurek, J.-D. Foulon, T. A. Hamor, C. J. Jones, J. A. McCleverty, S. M. Hubig, E. J. L. McInnes, N. N. Payne and L. J. Yellowlees, *Inorg. Chem.*, 1995, **34**, 4414.
6 N. M. Rowley, S. S. Kurek, P. R. Ashton, T. A. Hamor, C. J. Jones, N. Spencer, J. A. McCleverty, G. S. Beddard, T. M. Feehan, N. T. H. White, E. J. L. McInnes, N. N. Payne and L. J. Yellowlees, *Inorg. Chem.*, 1996, **35**, 5526.
7 M. T. Barton, N. M. Rowley, P. R. Ashton, C. J. Jones, N. Spencer, M. S. Tolley and L. J. Yellowlees, *New J. Chem.*, 2000, **24**, 555.
8 A. D. Adler, F. R. Longo, J. D. Finarelli, J. Goldmacher, J. Assour and L. Korsakoff, *J. Org. Chem.*, 1967, **32**, 476.
9 J.-H. Fuhrhop and K. M. Smith, *Laboratory Methods in Porphyrin and Metalloporphyrin Research*, Elsevier, Oxford, 1976.
10 D. G. Davis, in *The Porphyrins*, ed. D. Dolphin, Academic Press, New York, 1978, vol. 5, ch. 4.
11 M. Veyrat, R. Ramasseul, I. Turowska-Tyrk, W. R. Scheidt, M. Autret, K. M. Kadish and J.-C. Marchon, *Inorg. Chem.*, 1999, **38**, 1772.
12 D. Collison, F. E. Mabbs, E. J. L. McInnes, K. J. Taylor, A. J. Welch and L. J. Yellowlees, *J. Chem. Soc.*, *Dalton Trans.*, 1996, 329.
13 E. J. L. McInnes, R. D. Farley, C. C. Rowlands, A. J. Welch, L. Rovatti and L. J. Yellowlees, *J. Chem. Soc.*, *Dalton Trans.*, 1999, 4203.
14 WINEPR SimFonia, version 1.25, Bruker Analytische Messtechnik GmbH, 1996.
15 J. Homer and M. Perry, *J. Chem. Soc.*, *Chem. Commun.*, 1994, 373.